

IRIS : Interactive Responsive Intelligent Segmentation for 3D Affordance Analysis

Meng Chu¹, Xuan Zhang¹

Abstract—Recent advancements in large language and vision-language models have significantly enhanced multimodal understanding, yet translating high-level linguistic instructions into precise robotic actions in 3D space remains challenging. This paper introduces IRIS (Interactive Responsive Intelligent Segmentation), a novel training-free multimodal system for 3D affordance segmentation, alongside a benchmark for evaluating interactive language-guided affordance in everyday environments. IRIS integrates a large multimodal model with a specialized 3D vision network, enabling seamless fusion of 2D and 3D visual understanding with language comprehension. To facilitate evaluation, we present a dataset of 10 typical indoor environments, each with 50 images annotated for object actions and 3D affordance segmentation. Extensive experiments demonstrate IRIS’s capability in handling interactive 3D affordance segmentation tasks across diverse settings, showcasing competitive performance across various metrics. Our results highlight IRIS’s potential for enhancing human-robot interaction based on affordance understanding in complex indoor environments, advancing the development of more intuitive and efficient robotic systems for real-world applications.

I. INTRODUCTION

In the rapidly evolving field of robotics and computer vision, the ability to understand and interact with complex 3D environments remains a frontier ripe for exploration. Recent years have witnessed unprecedented advancements in artificial intelligence, particularly with the emergence of large language models (LLMs) and vision-language models [1], [2], [3]. These breakthroughs have revolutionized numerous aspects of AI, from natural language processing to image recognition. However, a significant challenge persists: bridging the gap between high-level linguistic instructions and precise 3D robotic actions in real-world scenarios [4], [5], [6].

The integration of language understanding with spatial reasoning and manipulation skills is crucial for the next generation of intelligent systems [7], [8]. While LLMs excel at processing and generating human-like text, and vision models can interpret complex visual scenes, translating this understanding into actionable 3D interactions remains an open problem. This challenge is particularly evident in embodied AI applications, where agents must navigate, manipulate, and interact with their physical surroundings based on natural language instructions [9], [10].

Traditional approaches in robotics and computer vision have often addressed 2D and 3D domains separately, lacking the holistic perspective necessary for effective embodied

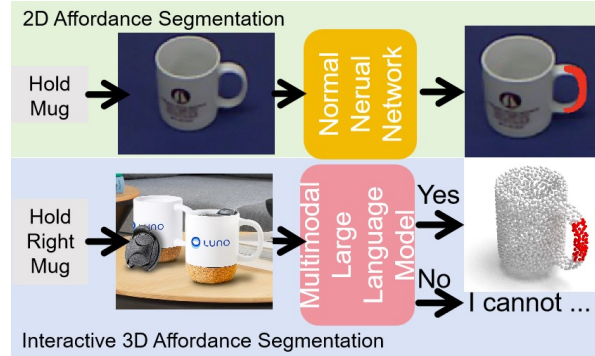


Fig. 1. Comparison of 2D Affordance Segmentation and interactive 3D Affordance Segmentation.

interaction [11], [12]. Two-dimensional visual understanding, while advanced, falls short in capturing the full complexity of real-world environments. Conversely, pure 3D approaches often struggle with semantic interpretation and language grounding [13], [14]. This dichotomy has limited the development of truly versatile and intuitive robotic systems capable of understanding and acting upon nuanced human instructions in diverse settings [15], [16].

Recent research has begun to explore the potential of LLMs in embodied navigation and planning tasks [17], [18]. These studies have shown promising results in high-level decision-making and route planning. However, they frequently encounter limitations when it comes to fine-grained manipulation tasks that demand precise spatial understanding and object interaction [19]. The ability to grasp the affordances of objects—their potential uses and interactions—in a 3D context while aligning with natural language instructions remains a significant hurdle [20].

To address these challenges, we propose IRIS (Interactive Responsive Intelligent Segmentation), a novel training-free multimodal framework. As shown in Fig. 1, IRIS is designed to bridge the gap between linguistic comprehension and 3D spatial understanding, enabling more intuitive and effective human-robot interaction. The core motivation behind IRIS stems from the need to equip embodied agents with the capability to seamlessly integrate 2D and 3D visual understanding with language comprehension [21].

Our framework leverages the strengths of large multimodal models, combining them with specialized networks to process and reason about visual and linguistic inputs in tandem [21], [22], [23]. This integration allows IRIS to perform

¹All authors are with School of Computing, National University of Singapore.

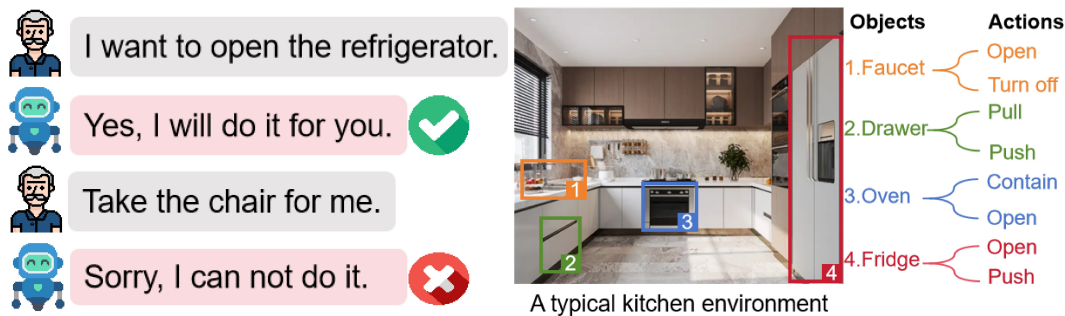


Fig. 2. Demonstration of IRIS Interactive Query-Answer Function and Possible Affordance Segmentation in a Typical Kitchen Environment.

sophisticated vision-language reasoning, translating high-level instructions into precise 3D affordance segmentation without additional training. By doing so, IRIS opens new possibilities for robots to understand and interact with their environment in ways that more closely align with human intentions and expectations [1], [4].

IRIS tackles these limitations by uniquely combining two effective components: a large multimodal model for vision-language understanding [24] and a specialized network for language-guided 3D affordance segmentation [25].

This integration enables IRIS to process multimodal inputs, perform vision-language understanding, localize objects, retrieve and register 3D point clouds, and execute language-guided 3D affordance segmentation—all without requiring additional training.

The key contributions of this work are as follows:

- We present a training-free multimodal system linking high-level instructions and precise robotic actions in 3D environments. Our IRIS framework introduces a novel pipeline that integrates 2D and 3D visual understanding with language comprehension for embodied agents, demonstrating state-of-the-art performance in 3D affordance analysis and segmentation across diverse indoor environments.
- We provide a new dataset specifically designed for evaluating interactive language-guided affordance segmentation in everyday environments. This dataset enables more comprehensive testing and development of multimodal systems for complex spatial understanding tasks.

II. RELATED WORK

Large Models for Visual Understanding. Large models have significantly trumped visual understanding tasks with the supervision of language [26], [27]. In 2D visual grounding, GPT4ROI [28] encodes region features interleaved with language embeddings for fine-grained multimodal reasoning. Shikra [29] further improves visual grounding in the unified natural language form. 3D environments bring out greater complexity but provide more precise details compared to 2D images. For 3D understanding, Chen et al. established ScanRefer [30] to learn the correlated representation between 3D object proposals and encoded description embeddings. Building on this, ScanQA [31] is formulated for 3D question

answering. However, these methods only focus on either 2D or 3D domains separately, lacking the holistic perspective for embodied agents. Our IRIS framework bridges this gap by seamlessly combining 2D and 3D visual understanding with language comprehension.

Embodied Agents for Robotic Tasks. Embodied agents in robotics aim to unify visual perception and physical action in real-world environments. To enable and encourage the application of situated multimodal learning, vision-and-language navigation [32] is first presented for embodied learning. Furthermore, Hong et al. [33] equips the BERT model recurrent functions to capture the cross-model time-aware information for agents. As the planning capability of Large Language Models (LLMs) has revolutionized the vision-language problem [34], [35], [36], some researchers attempt to apply LLMs as an auxiliary module for embodied navigation. Huang et al. [37] extends the powerful reasoning ability of LLMs grounding on embodied context and language feedback, while Singh et al. [38] structures program-like prompts to enable the universal plan generation across diverse situated tasks. Chen et al. [39] builds an online language-formed map to extend the agent action space from local to global. These works highlight the potential of language models in embodied robot planning, yet they often struggle with fine-grained manipulation that requires precise spatial understanding. Our paper addresses this limitation by integrating LLMs with 3D point cloud processing for highly accurate object interaction and manipulation.

Affordance Learning in Robotics. Affordance learning is crucial for robotic manipulation tasks. Traditional approaches like 3D AffordanceNet [40] focused on learning affordances by detecting objects in the end-to-end architecture. Yang et al. [41] extends this by proposing a setting for learning 3D affordance parts guided by image demonstrations, but discarding the semantic information. More recently, Li et al. [25] introduces PointRefer, a novel task for language-guided affordance segmentation on 3D objects. While these works have made significant strides in affordance detection, they often lack the flexibility to integrate with diverse, context-rich instructions under LLM generation. Our approach differs by directly learning from linguistic context, aligning more closely with the semantic richness of LLMs and their potential downstream applications in robotics.

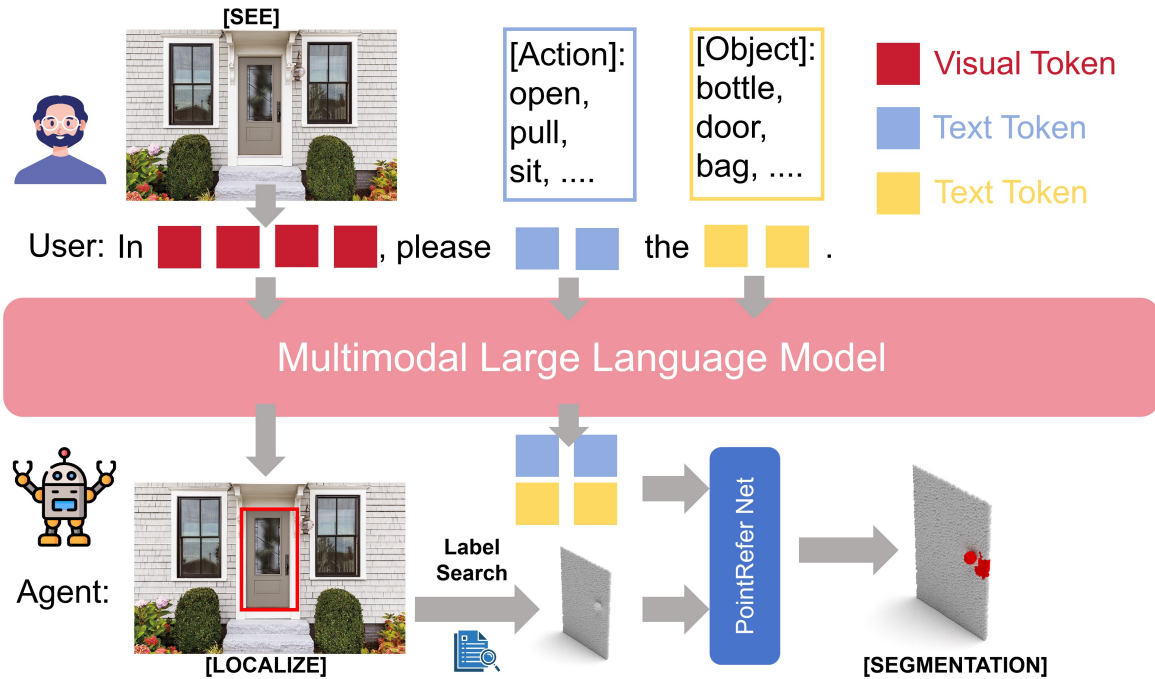


Fig. 3. Structure and Working Flow of IRIS System.

As shown in Fig. 2, humans typically perceive and communicate about their environment in 2D, while robots need to perform tasks in 3D spaces. IRIS bridges this gap by interpreting 2D visual information from humans and translating it into 3D actions for robots. This capability is crucial as robots become more integrated into our daily lives, from homes to factories.

III. METHODOLOGY

We present IRIS, a novel training-free multimodal system for advanced object understanding and interaction. Our approach integrates a large multimodal model [24] for vision-language understanding and a specialized network [25] for language-guided 3D affordance segmentation.

A. System Overview

Figure 3 illustrates a comprehensive system for language-guided robotic interactions, comprising several key stages. The process begins with multimodal input processing of visual and textual information, followed by vision-language understanding and object localization to interpret the input and identify relevant objects. Next, 3D point cloud retrieval and registration aligns 2D visual data with 3D spatial information. The fourth stage involves language-guided 3D affordance segmentation, determining how objects can be interacted with based on given instructions. Finally, 2D and 3D information are integrated for the final output, bridging the gap between high-level commands and precise robotic actions. This approach allows IRIS to understand complex instructions and translate them into actionable insights for robotic systems, enabling precise, language-guided interactions in 3D environments.

The vision-language understanding process in NExT-Chat involves two primary components: cross-modal attention computation and object localization and classification. Each of these components is represented by specific equations that warrant detailed explanation.

B. Cross-modal Attention Computation

The cross-modal attention mechanism, a key element in transformer-based models, is represented by the following equation:

$$A = \text{softmax} \left(\frac{QK^T}{\sqrt{d_k}} \right) V \quad (1)$$

where Q , K , and V denote Query, Key, and Value matrices, respectively. In cross-modal contexts, these may be derived from different modalities (e.g., Q from text, K and V from image features).

C. Object Localization and Classification

The object localization and classification process is represented by three distinct equations:

1) Localization Score:

$$L = \sigma(W_L F + b_L) \quad (2)$$

where F represents a feature vector extracted from the image, W_L and b_L are learned weight matrix and bias for localization, $\sigma(\cdot)$ denotes the sigmoid activation function, which constrains the output to a range between 0 and 1, L represents the localization score, indicating the likelihood of an object's presence.

2) Bounding Box Prediction:

$$B = W_B F + b_B \quad (3)$$

This equation is similar to the localization score equation but lacks an activation function. W_B and b_B are learned parameters for bounding box prediction, and B directly outputs the predicted bounding box coordinates.

3) Object Classification:

$$O = \arg \max(\text{softmax}(W_O F + b_O)) \quad (4)$$

where: W_O and b_O are learned parameters for object classification, $\text{softmax}(\cdot)$ normalizes the output into a probability distribution over object classes, $\arg \max(\cdot)$ selects the class with the highest probability, O represents the predicted object category.

D. Decision Module and Point Cloud Retrieval

Based on NExT-Chat’s output, the system performs the following steps:

1) Decision making:

$$D = f(R_{VL}, B, O) \quad (5)$$

where f is a decision function, outputting $D \in \{0, 1\}$ indicating whether to proceed to the next step.

2) If $D = 1$, the system retrieves the corresponding point cloud data from the database:

$$P = \text{Database}(O) \quad (6)$$

where P is the retrieved 3D point cloud data.

E. Language-Guided 3D Affordance Segmentation

PointRefer receives the output from the decision module and the retrieved point cloud P to perform language-guided affordance segmentation:

1) Adaptive Fusion Module (AFM):

$$F_{fused} = \text{AFM}(R_{VL}, P) \quad (7)$$

2) Referred Point Decoder (RPD) generates dynamic convolution kernels:

$$K_{dynamic} = \text{RPD}(F_{fused}) \quad (8)$$

3) 3D affordance segmentation:

$$M_{3D} = \sigma(K_{dynamic} * F_{fused}) \quad (9)$$

where M_{3D} is the final 3D affordance segmentation mask.

Through this comprehensive process, the IRIS system achieves end-to-end mapping from 2D images and text instructions to 3D affordance segmentation. The system’s innovation lies in combining powerful vision-language understanding capabilities, intelligent decision-making mechanisms, and precise 3D affordance segmentation techniques, enabling complex language instructions to be directly transformed into operational areas in 3D space.

IV. DATASET

We present a comprehensive dataset designed for evaluating interactive language-guided affordance segmentation in everyday environments, building upon the work of [25], [42]. Our dataset encompasses 10 diverse indoor settings commonly encountered in daily life, with each environment represented by 50 high-quality annotated images. These annotations include object bounding boxes, labels, 3D point cloud data, and affordance segmentation information. The query question from humans is made from GPT4 [43]. By integrating 2D image data with 3D point cloud representations and affordance segmentation, this dataset bridges the gap between high-level linguistic instructions and precise 3D affordance understanding. The dataset’s focus on everyday environments enhances its real-world applicability, making it particularly suitable for tasks involving language-guided robotic interactions in common indoor settings.

A. Dataset Structure and Annotation

Our dataset is structured around common household and workplace scenarios, each designed to test different aspects of embodied AI:

- 1) **Kitchen:** Includes objects like faucets, drawers, ovens, and refrigerators.
- 2) **Living Room:** Features furniture, electronics, and decorative items.
- 3) **Bedroom:** Contains sleep-related furniture and personal items.
- 4) **Office:** Focuses on work-related equipment and furniture.
- 5) **Entrance/Hallway:** Highlights transitional spaces and storage.
- 6) **Study Area:** Emphasizes learning environments and materials.
- 7) **Leisure Space:** Includes entertainment and relaxation items.
- 8) **Cleaning Area:** Features cleaning tools and appliances.
- 9) **Storage and Organization:** Focuses on storage solutions and personal belongings.
- 10) **Dining Area:** Includes dining furniture and tableware.

Each image in the dataset is meticulously annotated with: precise bounding boxes and its label for all relevant objects; detailed affordance segmentation masks for manipulable objects; object-action correspondences listing possible actions for each object; and natural language descriptions of possible tasks and interactions.

B. Affordance Segmentation for Embodied Agents

A key feature of our dataset is the inclusion of detailed affordance segmentation annotations. These annotations provide pixel-level information about how objects can be interacted with, crucial for embodied agents to understand and manipulate their environment. For example: **Faucet** is annotated with actions such as “Open”, “Turn off”, and “Pull”; **Drawer** is labeled with “Open” and “Push” affordances; **Oven** is segmented with “Contain” and “Open”

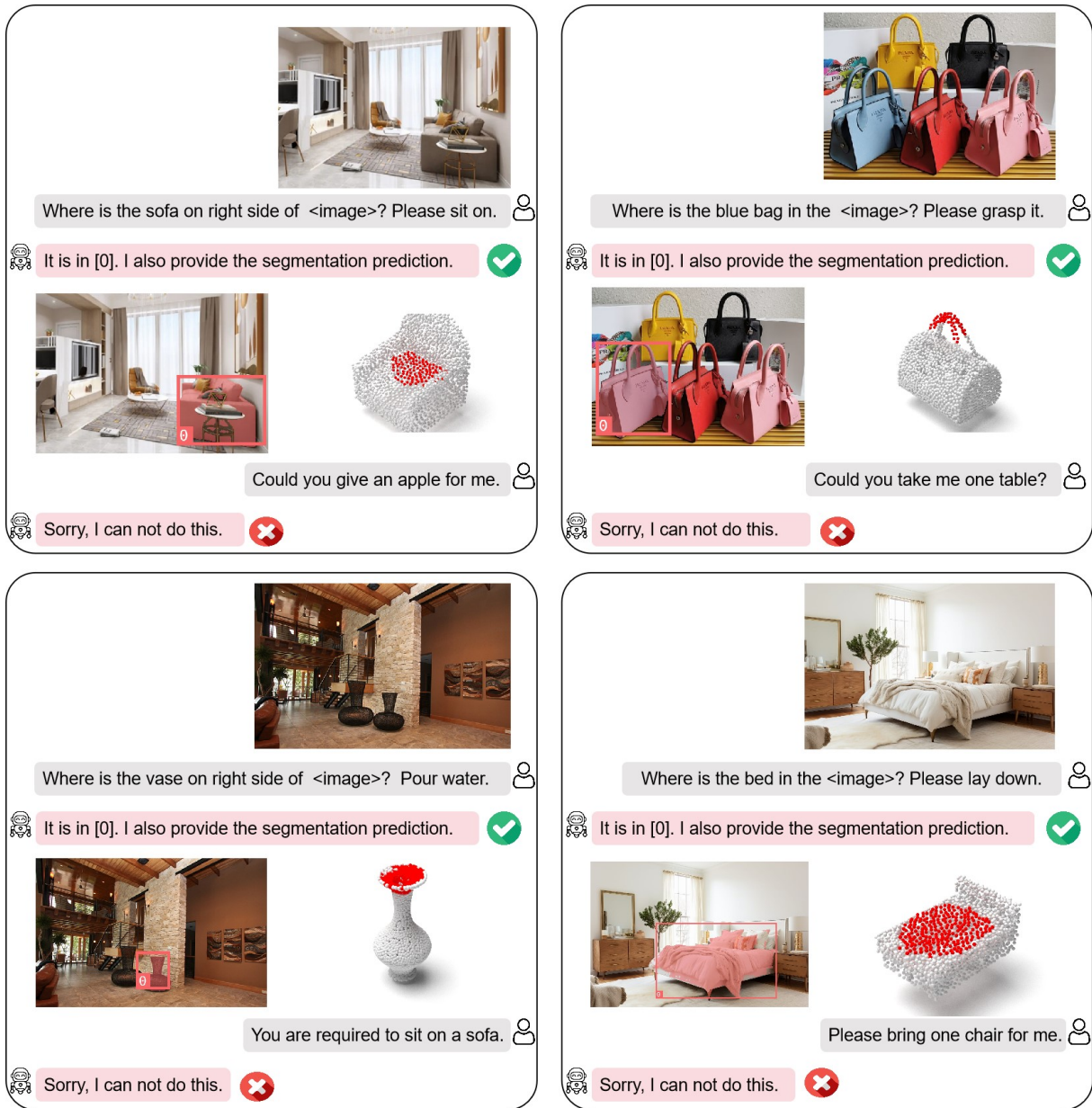


Fig. 4. Case-Study of IRIS's Interactive 3D segmentation.

functionalities; and **Refrigerator** is marked with “Open” and “Push” interactions.

This granular level of annotation allows for testing an agent’s ability to not just recognize objects, but to understand how to interact with them in context-appropriate ways.

V. EXPERIMENTS

To evaluate the effectiveness of our proposed IRIS system for 3D affordance analysis, we conducted extensive experiments comparing it with state-of-the-art methods and analyzing its performance across various indoor environments. This section details our experimental setup, quantitative results, qualitative analysis, and discussion of findings.

A. Experimental Setup

We evaluated IRIS on a diverse dataset of indoor environments, encompassing ten different room types commonly found in residential settings on one A100 GPU. The dataset includes a wide range of objects with various affordances to test the system’s capability in 3D affordance analysis and segmentation. Our experiments were designed to assess both the quantitative performance metrics and qualitative aspects of the system’s understanding and interaction capabilities.

B. Performance Metrics

We used four standard metrics to evaluate quantitative performance:

- **mIoU (mean Intersection over Union)**: Measures 3D segmentation accuracy.

TABLE I

PERFORMANCE COMPARISON OF DIFFERENT METHODS

Method	mIoU \uparrow	AUC \uparrow	SIM \uparrow	MAE \downarrow
GLIP[44] + ReferTrans [45]	11.5	75.3	0.414	0.135
GDINO[46] + ReferTrans [45]	12.7	77.6	0.425	0.131
Next-chat[24] + ReferTrans [45]	13.5	78.5	0.457	0.128
GLIP[44] + ReLa[47]	14.2	73.1	0.502	0.123
GDINO[46] + ReLa[47]	15.0	75.4	0.515	0.121
Next-chat[24] + ReLa[47]	15.8	76.5	0.525	0.118
GLIP[44] + IAGNet[41]	16.0	77.5	0.533	0.116
GDINO[46] + IAGNet[41]	16.7	79.4	0.537	0.114
Next-chat[24] + IAGNet[41]	17.3	80.3	0.544	0.113
GLIP[44] + PointRefer[25]	17.5	81.7	0.551	0.112
GDINO[46] + PointRefer[25]	18.2	82.0	0.575	0.105
IRIS (Ours)	19.2	83.1	0.603	0.098

- **AUC (Area Under the Curve):** Evaluates overall performance across different affordance detection thresholds.
- **SIM (Similarity):** Assesses similarity between predicted and ground truth 3D affordance segmentations.
- **MAE (Mean Absolute Error):** Measures average magnitude of affordance prediction errors in 3D space.

C. Quantitative Results

1) *Comparative Analysis:* Table I presents a comparison of IRIS with other state-of-the-art methods in 3D affordance analysis and segmentation.

IRIS outperforms all baseline methods across all metrics, with notable improvements: 19.2% in mIoU over the next best method with 1% higher. Highest AUC score of 83.1, indicating superior overall performance. The best SIM score was 0.603, demonstrating accurate 3D affordance segmentations. The lowest MAE of 0.098, highlighting precision in affordance localization.

2) *Performance Across Different environments:* Table II presents IRIS’s performance across ten different indoor environments.

Observations from the environment-specific performance data reveal consistent performance across all environments, with the mIoU range spanning from 18.3 to 19.9. IRIS demonstrates its best performance in structured environments, achieving an mIoU of 19.9 in kitchen environments and 19.7 in dining areas. Notably, the system maintains robust performance even in challenging environments, as evidenced by the mIoU of 18.3 in entrance/hallway environments, which often present complex spatial arrangements and diverse object types. Other metrics also show this trend.

D. Qualitative Results

To complement our quantitative results, we conducted a qualitative analysis of IRIS’s performance across various scenarios, as illustrated in Fig. 4. IRIS demonstrates strong performance in diverse environments, accurately identifying and segmenting objects such as a sofa in a living room environment, a blue bag among multiple bags, a vase in an entrance area, and a bed in a bedroom environment. The system shows a good grasp of object affordances, associating

TABLE II

IRIS PERFORMANCE ACROSS DIFFERENT ENVIRONMENTS

Environment	mIoU \uparrow	AUC \uparrow	SIM \uparrow	MAE \downarrow
Kitchen	19.9	84.1	0.613	0.095
Living Room	19.5	83.4	0.606	0.097
Bedroom	18.9	82.8	0.599	0.099
Office	19.6	83.7	0.610	0.096
Entrance/Hallway	18.3	82.0	0.592	0.102
Study Area	19.3	83.2	0.604	0.098
Leisure Space	19.1	82.9	0.601	0.100
Cleaning Area	18.6	82.3	0.595	0.101
Storage and Organization	18.8	82.6	0.597	0.100
Dining Area	19.7	83.9	0.612	0.095
Average	19.2	83.1	0.603	0.098

“sit on” with the sofa, recognizing the “grasp” affordance for the blue bag, understanding the “pour water” action for the vase, and correctly interpreting the “lay down” affordance for the bed. IRIS generates accurate 3D point cloud representations of segmented objects, capturing their shape and structure, which is crucial for potential applications in robotics and augmented reality. The qualitative results also reveal IRIS’s interactive function. It correctly identifies its inability to perform physical actions (e.g., giving an apple, taking a table). It demonstrates an understanding of its role as an analysis and segmentation system, not a physical actor.

E. Discussion

The experimental results demonstrate IRIS’s superior performance in 3D affordance analysis and segmentation tasks. The system exhibits environment versatility, maintaining high performance across various indoor environments, from structured environments like kitchens to more challenging areas like hallways. Future work could explore IRIS’s performance in even more challenging scenarios, investigate potential enhancements for handling dynamic environments, and explore integration with robotic systems for physical interaction based on the affordance analysis provided by IRIS.

VI. CONCLUSION

This paper presents two main contributions to 3D affordance analysis and segmentation. First, we introduce IRIS, a novel training-free multimodal system that bridges high-level instructions and precise robotic actions in 3D environments. IRIS integrates 2D and 3D visual understanding with language comprehension, demonstrating competitive performance across diverse indoor settings. Second, we provide a new dataset for evaluating interactive language-guided affordance segmentation in everyday environments, enabling comprehensive testing of multimodal systems for complex spatial understanding tasks. By combining sophisticated visual-language processing with precise 3D affordance segmentation, these contributions advance embodied AI applications and enhance human-robot interactions in real-world scenarios, paving the way for more capable and responsive robotic systems

REFERENCES

- [1] M. J. Kim, K. Pertsch, S. Karamcheti, T. Xiao, A. Balakrishna, S. Nair, R. Rafailov, E. Foster, G. Lam, P. Sanketi, *et al.*, “Open-vla: An open-source vision-language-action model,” *arXiv preprint arXiv:2406.09246*, 2024.
- [2] C. Wei and Z. Deng, “Incorporating scene graphs into pre-trained vision-language models for multimodal open-vocabulary action recognition,” in *2024 IEEE International Conference on Robotics and Automation (ICRA)*. IEEE, 2024, pp. 440–447.
- [3] Y. Hong, M. J. Kim, I. Lee, and S. B. Yoo, “Fluxformer: Flow-guided duplex attention transformer via spatio-temporal clustering for action recognition,” *IEEE Robotics and Automation Letters*, 2023.
- [4] S. Chen, R. G. Pinel, C. Schmid, and I. Laptev, “Polarnet: 3d point clouds for language-guided robotic manipulation,” in *Conference on Robot Learning*. PMLR, 2023, pp. 1761–1781.
- [5] G. Tziafas, Y. Xu, A. Goel, M. Kasaei, Z. Li, and H. Kasaei, “Language-guided robot grasping: Clip-based referring grasp synthesis in clutter,” *arXiv preprint arXiv:2311.05779*, 2023.
- [6] M. Ahn, A. Brohan, N. Brown, Y. Chebotar, O. Cortes, B. David, C. Finn, C. Fu, K. Gopalakrishnan, K. Hausman, *et al.*, “Do as i can, not as i say: Grounding language in robotic affordances,” *arXiv preprint arXiv:2204.01691*, 2022.
- [7] H. Ha, P. Florence, and S. Song, “Scaling up and distilling down: Language-guided robot skill acquisition,” in *Conference on Robot Learning*. PMLR, 2023, pp. 3766–3777.
- [8] R. Zhang, S. Lee, M. Hwang, A. Hiranaka, C. Wang, W. Ai, J. J. R. Tan, S. Gupta, Y. Hao, G. Levine, *et al.*, “Noir: Neural signal operated intelligent robots for everyday activities,” *arXiv preprint arXiv:2311.01454*, 2023.
- [9] W. Xia, D. Wang, X. Pang, Z. Wang, B. Zhao, D. Hu, and X. Li, “Kinematic-aware prompting for generalizable articulated object manipulation with llms,” in *2024 IEEE International Conference on Robotics and Automation (ICRA)*. IEEE, 2024, pp. 2073–2080.
- [10] Z. Zhou, J. Song, K. Yao, Z. Shu, and L. Ma, “Isr-llm: Iterative self-refined large language model for long-horizon sequential task planning,” in *2024 IEEE International Conference on Robotics and Automation (ICRA)*. IEEE, 2024, pp. 2081–2088.
- [11] B. Xing, X. Ying, and R. Wang, “Masked local-global representation learning for 3d point cloud domain adaptation,” in *2024 IEEE International Conference on Robotics and Automation (ICRA)*. IEEE, 2024, pp. 418–424.
- [12] K. Vidanapathirana, P. Moghadam, S. Sridharan, and C. Fookes, “Spectral geometric verification: Re-ranking point cloud retrieval for metric localization,” *IEEE Robotics and Automation Letters*, vol. 8, no. 5, pp. 2494–2501, 2023.
- [13] C. Liu, G. Chen, and R. Song, “Lps-net: Lightweight parameter-shared network for point cloud-based place recognition,” in *2024 IEEE International Conference on Robotics and Automation (ICRA)*. IEEE, 2024, pp. 448–454.
- [14] B. Wang, W. Li, B. Zhang, and Y. Liu, “Joint response and background learning for uav visual tracking,” in *2024 IEEE International Conference on Robotics and Automation (ICRA)*. IEEE, 2024, pp. 455–462.
- [15] P. Ausserlechner, D. Habegger, S. Thalhammer, J.-B. Weibel, and M. Vincze, “Zs6d: Zero-shot 6d object pose estimation using vision transformers,” in *2024 IEEE International Conference on Robotics and Automation (ICRA)*. IEEE, 2024, pp. 463–469.
- [16] M. Chu, Z. Cui, A. Zhang, J. Yao, C. Tang, Z. Fu, A. Nathan, and S. Gao, “Multisensory fusion, haptic, and visual feedback teleoperation system under iot framework,” *IEEE Internet of Things Journal*, vol. 9, no. 20, pp. 19717–19727, 2022.
- [17] D. Shah, B. Osiniński, b. ichter, and S. Levine, “Lm-nav: Robotic navigation with large pre-trained models of language, vision, and action,” in *Proceedings of The 6th Conference on Robot Learning*, ser. Proceedings of Machine Learning Research, K. Liu, D. Kulic, and J. Ichnowski, Eds., vol. 205. PMLR, 14–18 Dec 2023, pp. 492–504.
- [18] D. Shah, M. R. Equi, B. Osiniński, F. Xia, B. Ichter, and S. Levine, “Navigation with large language models: Semantic guesswork as a heuristic for planning,” in *Conference on Robot Learning*. PMLR, 2023, pp. 2683–2699.
- [19] X. Long, H. Zhao, C. Chen, F. Gu, and Q. Gu, “A novel wide-area multiobject detection system with high-probability region searching,” *arXiv preprint arXiv:2405.04589*, 2024.
- [20] S. Lu, H. Chang, E. P. Jing, A. Boularias, and K. Bekris, “Ovir-3d: Open-vocabulary 3d instance retrieval without training on 3d data,” in *Conference on Robot Learning*. PMLR, 2023, pp. 1610–1620.
- [21] B. Zitkovich, T. Yu, S. Xu, P. Xu, T. Xiao, F. Xia, J. Wu, P. Wohlhart, S. Welker, A. Wahid, *et al.*, “Rt-2: Vision-language-action models transfer web knowledge to robotic control,” in *Conference on Robot Learning*. PMLR, 2023, pp. 2165–2183.
- [22] S. Saxena, M. Sharma, and O. Kroemer, “Multi-resolution sensing for real-time control with vision-language models,” in *Conference on Robot Learning*. PMLR, 2023, pp. 2210–2228.
- [23] M. Chu, Z. Zheng, W. Ji, T. Wang, and T.-S. Chua, “Towards natural language-guided drones: Geotext-1652 benchmark with spatial relation matching,” in *Proceedings of the European Conference on Computer Vision (ECCV)*, 2024.
- [24] A. Zhang, Y. Yao, W. Ji, Z. Liu, and T.-S. Chua, “Next-chat: An lmm for chat, detection and segmentation,” in *Forty-first International Conference on Machine Learning*, 2024.
- [25] Y. Li, N. Zhao, J. Xiao, C. Feng, X. Wang, and T.-s. Chua, “Laso: Language-guided affordance segmentation on 3d object,” in *Proceedings of the IEEE/CVF Conference on Computer Vision and Pattern Recognition (CVPR)*, June 2024, pp. 14251–14260.
- [26] S. Huang, L. Dong, W. Wang, Y. Hao, S. Singhal, S. Ma, T. Lv, L. Cui, O. K. Mohammed, B. Patra, *et al.*, “Language is not all you need: Aligning perception with language models,” *Advances in Neural Information Processing Systems*, vol. 36, pp. 72096–72109, 2023.
- [27] J. Li, D. Li, S. Savarese, and S. Hoi, “Blip-2: Bootstrapping language-image pre-training with frozen image encoders and large language models,” in *International conference on machine learning*. PMLR, 2023, pp. 19730–19742.
- [28] S. Zhang, P. Sun, S. Chen, M. Xiao, W. Shao, W. Zhang, Y. Liu, K. Chen, and P. Luo, “Gpt4roi: Instruction tuning large language model on region-of-interest,” *arXiv preprint arXiv:2307.03601*, 2023.
- [29] K. Chen, Z. Zhang, W. Zeng, R. Zhang, F. Zhu, and R. Zhao, “Shikra: Unleashing multimodal llm’s referential dialogue magic,” *arXiv preprint arXiv:2306.15195*, 2023.
- [30] D. Z. Chen, A. X. Chang, and M. Nießner, “Scanrefer: 3d object localization in rgb-d scans using natural language,” in *European Conference on Computer Vision*. Springer, 2020, pp. 202–221.
- [31] D. Azuma, T. Miyanishi, S. Kurita, and M. Kawanabe, “Scanqa: 3d question answering for spatial scene understanding,” in *proceedings of the IEEE/CVF conference on computer vision and pattern recognition*, 2022, pp. 19129–19139.
- [32] P. Anderson, Q. Wu, D. Teney, J. Bruce, M. Johnson, N. Sünderhauf, I. Reid, S. Gould, and A. Van Den Hengel, “Vision-and-language navigation: Interpreting visually-grounded navigation instructions in real environments,” in *Proceedings of the IEEE conference on computer vision and pattern recognition*, 2018, pp. 3674–3683.
- [33] Y. Hong, Q. Wu, Y. Qi, C. Rodriguez-Opazo, and S. Gould, “A recurrent vision-and-language bert for navigation,” *arXiv preprint arXiv:2011.13922*, 2020.
- [34] T. B. Brown, “Language models are few-shot learners,” *arXiv preprint arXiv:2005.14165*, 2020.
- [35] H. Touvron, T. Lavril, G. Izacard, X. Martinet, M.-A. Lachaux, T. Lacroix, B. Rozière, N. Goyal, E. Hambro, F. Azhar, *et al.*, “Llama: Open and efficient foundation language models,” *arXiv preprint arXiv:2302.13971*, 2023.
- [36] A. Q. Jiang, A. Sablayrolles, A. Mensch, C. Bamford, D. S. Chaplot, D. d. l. Casas, F. Bressand, G. Lengyel, G. Lample, L. Saulnier, *et al.*, “Mistral 7b,” *arXiv preprint arXiv:2310.06825*, 2023.
- [37] W. Huang, F. Xia, T. Xiao, H. Chan, J. Liang, P. Florence, A. Zeng, J. Tompson, I. Mordatch, Y. Chebotar, *et al.*, “Inner monologue: Embodied reasoning through planning with language models,” *arXiv preprint arXiv:2207.05608*, 2022.
- [38] I. Singh, V. Blukis, A. Mousavian, A. Goyal, D. Xu, J. Tremblay, D. Fox, J. Thomason, and A. Garg, “Progprompt: Generating situated robot task plans using large language models,” in *2023 IEEE International Conference on Robotics and Automation (ICRA)*. IEEE, 2023, pp. 11523–11530.
- [39] J. Chen, B. Lin, R. Xu, Z. Chai, X. Liang, and K.-Y. K. Wong, “Mapgpt: Map-guided prompting for unified vision-and-language navigation,” *arXiv preprint arXiv:2401.07314*, 2024.
- [40] T.-T. Do, A. Nguyen, and I. Reid, “Affordancenet: An end-to-end deep learning approach for object affordance detection,” in *2018 IEEE international conference on robotics and automation (ICRA)*. IEEE, 2018, pp. 5882–5889.

- [41] Y. Yang, W. Zhai, H. Luo, Y. Cao, J. Luo, and Z.-J. Zha, "Grounding 3d object affordance from 2d interactions in images," in *Proceedings of the IEEE/CVF International Conference on Computer Vision*, 2023, pp. 10 905–10 915.
- [42] S. Deng, X. Xu, C. Wu, K. Chen, and K. Jia, "3d affordancenet: A benchmark for visual object affordance understanding," in *proceedings of the IEEE/CVF conference on computer vision and pattern recognition*, 2021, pp. 1778–1787.
- [43] J. Achiam, S. Adler, S. Agarwal, L. Ahmad, I. Akkaya, F. L. Aleman, D. Almeida, J. Altenschmidt, S. Altman, S. Anadkat, *et al.*, "Gpt-4 technical report," *arXiv preprint arXiv:2303.08774*, 2023.
- [44] L. H. Li, P. Zhang, H. Zhang, J. Yang, C. Li, Y. Zhong, L. Wang, L. Yuan, L. Zhang, J.-N. Hwang, K.-W. Chang, and J. Gao, "Grounded language-image pre-training," in *Proceedings of the IEEE/CVF Conference on Computer Vision and Pattern Recognition (CVPR)*, June 2022, pp. 10 965–10 975.
- [45] M. Li and L. Sigal, "Referring transformer: A one-step approach to multi-task visual grounding," *Advances in neural information processing systems*, vol. 34, pp. 19 652–19 664, 2021.
- [46] S. Liu, Z. Zeng, T. Ren, F. Li, H. Zhang, J. Yang, C. Li, J. Yang, H. Su, J. Zhu, *et al.*, "Grounding dino: Marrying dino with grounded pre-training for open-set object detection," *arXiv preprint arXiv:2303.05499*, 2023.
- [47] C. Liu, H. Ding, and X. Jiang, "Gres: Generalized referring expression segmentation," in *Proceedings of the IEEE/CVF conference on computer vision and pattern recognition*, 2023, pp. 23 592–23 601.